RSC Sustainability

ROYAL SOCIETY OF CHEMISTRY

PERSPECTIVE

View Article Online
View Journal | View Issue

Cite this: *RSC Sustainability*, 2025, **3**, 4426

Perspective on electrochemical CO_2 reduction in CO_2/O_2 mixed gas

Xiaoling Lai, [a] Jinxian Feng, [a] Yuxuan Xiao, [a] Weng Fai Ip [*b] and Hui Pan [*ab]

Received 11th May 2025
Accepted 24th July 2025

DOI: 10.1039/d5su00334b

rsc.li/rscsus

Electrochemical CO_2 reduction reaction (CO_2RR) is a promising avenue to realize carbon neutrality. As the high-purity CO_2 in CO_2RR may diminish the feasibility and economic viability, the direct conversion of CO_2 in O_2-containing feed gas (CO_2/O_2) presents an attractive option. However, high CO_2RR kinetic barriers and the challenges associated with O_2 reduction significantly hamper the effectiveness of CO_2RR. Therefore, enhancing the selective CO_2RR in CO_2–O_2 mixed gas is critical. In this perspective, we first discuss factors of selective CO_2RR in CO_2/O_2. Then, state-of-the-art interface design strategies for the selective CO_2RR, including O_2 passivation, selective CO_2 adsorption and direct selective CO_2RR, are highlighted. Finally, a brief discussion on the current challenges and outlook for future directions to achieve highly efficient and O_2-tolerant CO_2RR systems are presented.

Sustainability spotlight

To realize the goal of a carbon-neutral society, converting excess CO_2 into valuable chemicals/fuels by biological, photochemical and electrochemical approaches has been extensively investigated. Electrochemical CO_2 reduction reaction (CO_2RR) driven by renewable electricity is a promising avenue to catalyze CO_2 into high value-added products. As the high-purity CO_2 in CO_2RR may diminish the feasibility and economic viability, the direct conversion of CO_2 in O_2-containing feed gas (CO_2/O_2) presents an attractive option, which can reduce the costs of CO_2 purification greatly. However, high CO_2RR kinetic barriers and the challenges associated with O_2 reduction significantly hamper the effectiveness of CO_2RR. Therefore, it is essential to enhance the O_2 tolerance of CO_2RR systems.

1 Introduction

Global economic growth and human activities significantly increase the CO_2 concentration in the atmosphere, leading to serious environmental problems, such as global warming, sea level rising and extreme climate.[1–6] Converting the excess CO_2 into valuable chemicals/fuels by biological,[7,8] photochemical[9,10] and electrochemical approaches[11–15] has been extensively investigated.[16,17] Among them, electrochemical CO_2 reduction reaction (CO_2RR) driven by renewable electricity has been emerging as a promising way toward carbon neutrality through catalyzing CO_2 into high value-added products.[18–24] At present, most CO_2RR systems utilize pure CO_2 as feedstock. However, the costs associated with CO_2 purification are significant, diminishing the economic benefits.[25,26]

The majority of human-induced CO_2 comes from flue gas (CO_2/O_2), therefore, the direct use of flue gas for feedstock of CO_2RR can reduce the costs of CO_2 purification and represent a potential strategy for CO_2RR applications. However, CO_2/O_2 reduction is facing a few challenging issues: (i) dilute CO_2 concentrations in CO_2/O_2, making the CO_2RR kinetics sluggish, and (ii) energetically favorable O_2 reduction reaction (ORR).[27] It has been clarified that only 5% O_2 in CO_2 inhibits CO_2RR completely.[28–30] Therefore, it is essential to enhance the O_2 tolerance of CO_2RR systems.[31] To date, challenges of flue gas reduction such as low transformation efficiency and unavoidable ORR persist although the coupling between direct flue gas utilization and electrochemical conversion has been investigated.[32] Thus, improving conversion efficiency is still the largest obstacle for the selective CO_2RR by using flue gas.

In recent years, numerous reviews have reported the electrochemical reduction of low-concentration CO_2 or CO_2-containing gas mixtures with impurities. For instance, Wang *et al.* systematically analyzed the scientific challenges and innovative strategies for the direct electrochemical conversion of CO_2 derived from industrial flue gases.[33] Similarly, Li *et al.* reviewed key design strategies for CO_2RR under dilute CO_2 conditions and in the presence of common gas impurities.[34] Despite O_2 being the most abundant impurity in industrial flue gas, with the O_2/CO_2 ratio being even greater than 20%, they just paid less attention to the selective CO_2/O_2 reduction in mixed gas systems. Therefore, the possible promotion effects of O_2 on CO_2RR and potential strategies should be carefully considered in the design of catalysts, electrode structures and electrolyte compositions, and this is an important area of research that should be focused on in the recent future.

[a]*Institute of Applied Physics and Materials Engineering, University of Macau, Macao SAR 999708, P. R. China. E-mail: huipan@um.edu.mo; Fax: +853-88222454; Tel: +853 88224427*

[b]*Department of Physics and Chemistry, Faculty of Science and Technology, University of Macau, Macao SAR 999078, P. R. China. E-mail: andyip@um.edu.mo*

In this perspective, we discuss the selective CO_2RR on different systems using flue gas as feedstock, which is expected to provide insight into O_2-tolerant CO_2RR. Firstly, the factors of CO_2/O_2 selective reduction performance are discussed. Then, strategies for designing the electrocatalytic reaction interface, such as surface modification that hampers O_2 transportation and enhances selective CO_2 adsorption or direct selective CO_2RR, are discussed. Finally, the current challenges in achieving high O_2-tolerant CO_2RR performance and insights into realizing large-scale applications in the future are summarized. We hope that this perspective shall illuminate the pathways toward developing excellent O_2-tolerant CO_2 electrocatalytic systems through the exploration of recent advances.

2 Factors affecting CO_2/O_2 selective reduction performance

The volume concentration of CO_2 in flue gas emission varies between 5% and 35%, typically around 15%.[35–38] Furthermore, flue gas contains impurities, such as O_2 and balancing inert N_2.[39] Considering that N_2 is hardly involved in the cathode reaction, the reduction of flue gas could be considered as CO_2/O_2 selective reduction. The solubility of CO_2 in water is only 1.45 g L^{-1} (273 K, 1 atm), indicating the limited concentration of CO_2 for CO_2RR. At the same time, CO_2RR is a complex process because of the multistep proton-electron transfer reactions as well as a variety of reaction paths. During the electrochemical reduction process, non-spontaneous electron transfer reactions are driven by an external power supply. The categories of CO_2RR products mainly depend on the externally applied potentials and catalysts, as well as electrolyte composition (eqn (1)–(11) (*E vs.* SHE)). Most CO_2RR systems still suffer from low Faraday Efficiency (FE) due to the competitive hydrogen evolution reaction (HER) (eqn (12) (*E vs.* SHE)) and multiple products (Fig. 1a). Importantly, ORR may also occur in flue gas reduction because it is thermodynamically more favorable than that of CO_2RR (eqn (13) and (14) (*E vs.* SHE)), suppressing CO_2RR simultaneously (Fig. 1b).

$$CO_2 + e^- \rightarrow CO_2^- \; E = -1.900 \text{ V} \quad (1)$$

$$CO_2 + 2H^+ + 2e^- \rightarrow HCOOH \; E = -0.610 \text{ V} \quad (2)$$

$$CO_2 + 2H^+ + 2e^- \rightarrow CO + H_2O \; E = -0.530 \text{ V} \quad (3)$$

$$2CO_2 + 2H^+ + 2e^- \rightarrow H_2C_2O_4 \; E = -0.913 \text{ V} \quad (4)$$

$$CO_2 + 4H^+ + 4e^- \rightarrow HCHO + H_2O \; E = -0.480 \text{ V} \quad (5)$$

$$CO_2 + 6H^+ + 6e^- \rightarrow CH_3OH + H_2O \; E = -0.380 \text{ V} \quad (6)$$

$$CO_2 + 8H^+ + 8e^- \rightarrow CH_4 + 2H_2O \; E = -0.240 \text{ V} \quad (7)$$

$$CO_2 + 12H^+ + 12e^- \rightarrow C_2H_4 + 4H_2O \; E = -0.349 \text{ V} \quad (8)$$

$$2CO_2 + 12H^+ + 12e^- \rightarrow C_2H_5OH + 3H_2O \; E = -0.329 \text{ V} \quad (9)$$

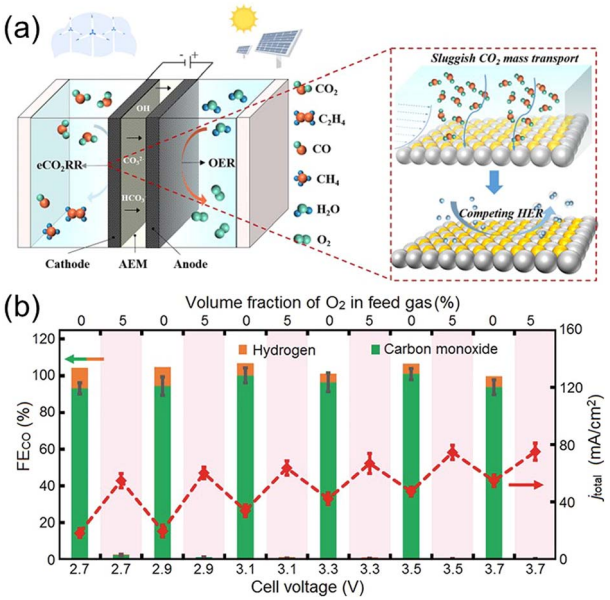

Fig. 1 (a) A typical design concept of a CO_2RR system. Sluggish CO_2 mass transport and competitive HER constitute two fundamental challenges in CO_2RR, especially for dilute CO_2 concentrations. (b) Faraday efficiency for CO production (FE_{CO}), FE_{H2} and total geometric current density (j_{total}) *vs.* cell voltage with and without O_2 in the feed gas. Compared to pure CO_2 feed (white background), the O_2-incorporated system (5 vol% O_2/CO_2, pink background) shows near-zero FE_{CO} and FE_{H2}, indicating complete dominance of O_2 reduction at this low ratio. The higher current density under O_2 is attributed to faster O_2 reduction kinetics *versus* CO_2RR. (a) Reproduced with permission.[40] Copyright 2024, Elsevier. (b) Reproduced with permission.[41] Copyright 2019, Elsevier.

$$2CO_2 + 14H^+ + 14e^- \rightarrow C_2H_6 + 4H_2O \; E = -0.270 \text{ V} \quad (10)$$

$$3CO_2 + 18H^+ + 18e^- \rightarrow C_3H_7OH + 5H_2O \; E = -0.310 \text{ V} \quad (11)$$

$$2H^+ + e^- \rightarrow H_2 \; E = -0.420 \text{ V} \quad (12)$$

$$O_2 + 2H^+ + 2e^- \rightarrow H_2O_2 \; E = 0.695 \text{ V} \quad (13)$$

$$O_2 + 4H^+ + 4e^- \rightarrow 2H_2O \; E = 1.229 \text{ V} \quad (14)$$

The electrocatalytic reaction happens at the solid–liquid–gas interface. Therefore, the design of the electrocatalyst–electrolyte interface is critical for selective CO_2RR. By rationally designing the catalyst and optimizing electrocatalytic conditions, the following factors can be effectively leveraged to manipulate the reaction process and improve the activity and selectivity of CO_2RR: (i) catalyst structure: surface active sites with specific element composition, crystallinity, defects, *etc.* can efficiently capture and enrich CO_2 to achieve high catalytic activity, selectivity and stability, by creating a low-O_2 environment through filtering out the O_2 molecules, or facilitating the conversion of key intermediates in CO_2RR in the presence of O_2. (ii) Electrolyte: electrolyte is another key component of CO_2RR systems, which includes the main electrolyte and additives,

including cations, anions and small organic molecules. Cations and anions in the electrolyte that affect the pH value within the solid–liquid structure have a significant influence on the electrochemical reactivity by tuning the structure of the electrical double layer. Additionally, the reactants and intermediates may also dynamically interact with the solvent molecules and additives in the electrolyte at the interface, altering the electrochemical reactivity and selectivity.

3 Strategies for CO_2/O_2 selective reduction

There have been a lot of strategies for improving the selectivity and activity of CO_2RR by adjusting the catalyst structure with O_2^- containing feed gas. Optimizing the CO_2/O_2 ratio on the catalyst shall be an effective strategy for CO_2/O_2 selective reduction, which could be achieved by O_2 passivation, selective CO_2 adsorption, and direct selective CO_2RR.

3.1 O_2 passivation strategy

The O_2 passivation strategy can enhance the selective CO_2RR by directly or indirectly slowing down O_2 transport. Introducing hydrophilic nanopores with sluggish O_2 transport and constructing a selective penetration layer with the O_2 prohibition ability can effectively slow down O_2 transport for efficient CO_2RR using flue gas.

3.1.1 Hydrophilic nanopores. CO_2 exhibits Lewis acidity due to the electrophilic carbon atom capable of accepting electron pairs, while O_2 is a non-polar molecule with minimal interaction with hydrophilic environments. Therefore, hydrophilic nanopore networks can selectively reduce O_2 mass flux to electrocatalytic centers by leveraging polarity-driven adsorption and size exclusion effects, thereby enhancing the efficiency and selectivity of CO_2 conversion.[42,43] Adding TiO_2 with hydrophilic nanopores on Cu catalysts can separate the O_2 and achieve good CO_2RR selectivity. Xu and co-workers[44] developed a catalyst composed of an ionomer with hydrophilic nanopores and TiO_2 nanoparticles as support particles and Cu as the main electrocatalyst (Fig. 2). The ionomer layer slowed down the O_2 transport rate to the catalyst and enabled a more efficient conversion of CO_2 to C_2 products with a FE_{C2} of 68% and a non-*iR*-corrected full cell energetic efficiency of 26%.

3.1.2 Selective penetration layer. Constructing an O_2 selective penetration layer could also improve CO_2RR selectivity by limiting O_2 penetration. Efficient O_2 selective penetration layers include: (1) specific frameworks with reversible photoswitching built to modulate the electron transfer rate and oxygen activation ability, and (2) microporous polymers with size-selective pores to filter O_2 and permeate CO_2 selectively. Zhu *et al.*[45] presented an O_2 passivation strategy to realize efficient CO_2RR performance by feeding CO_2/O_2 (a high FE_{CO} of 90.5% with a j_{CO} of -20.1 mA cm^{-2} at -1.0 V *vs.* RHE) under UV/Vis irradiation, and using the photoswitching built block 1,2-bis(5′-formyl-2′-methylthien-3′-yl) cyclopentene (DAE) in the material (Fig. 3a–e). DAE reversibly modulates the electrical conductivity and O_2 activation capacity by the framework ring-closing/opening reactions. Specifically, upon irradiation with UV, the close-DAE-BPy-CoPor exhibits higher electronic conductivity than open-DAE-BPy-CoPor (under Vis irradiation) because of the strong charge delocalization in close-DAE moieties. Furthermore, density functional theory (DFT) calculations and *operando* ATR-FTIR experiments demonstrated that the excellent CO_2RR performance of close-DAE-BPy-CoPor in co-feeding CO_2 and O_2 is attributed to the weak O_2 activation ability and high O_2 into *OOH (the ORR limiting step) free energy, thus resulting in the excellent selective CO_2RR performance in the presence of O_2.

CO_2 enrichment by physical pore confinement can also achieve highly selective electrochemical CO_2 reduction under an aerobic environment. For example, inspired by the natural photosynthesis unit, Lu's group[41] designed a PIM-CoPc/CNT hybrid electrode as an "artificial leaf" to enrich CO_2 in the presence of O_2 (Fig. 3f–h), where the PIM layer played a pivotal role in realizing CO_2/O_2 selective reduction. Serving as a molecular sieve with high gas permeability, the PIM layer effectively filters O_2 based on the molecular size and enriches CO_2 from the feed gas, and thus creates a low-O_2 local environment for the catalyst to achieve effective electrochemical CO_2-to-CO conversion. With 5% O_2 in the CO_2 feed gas, a FE_{CO} of 75.9% with a j_{total} of 27.3 mA cm^{-2} was achieved at a cell voltage of 3.1 V. Notably, an average CO_2/O_2 selectivity of ~20 suggested that 95% O_2 in the feed gas was rejected by the PIM layer.

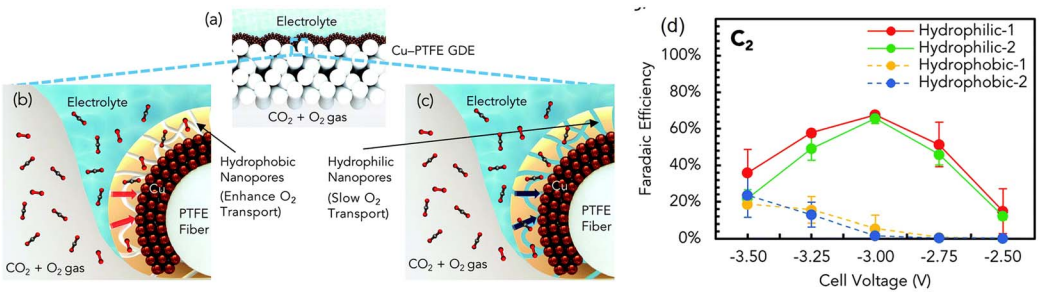

Fig. 2 (a) Schematic illustration of the Cu-PTFE GDE. Schematic of the GDE coated with the (b) hydrophobic and (c) hydrophilic nanoporous ionomer. (d) The FE toward C_2 products for different ionomers. Reproduced with permission.[44] Copyright 2020, The Royal Society of Chemistry.

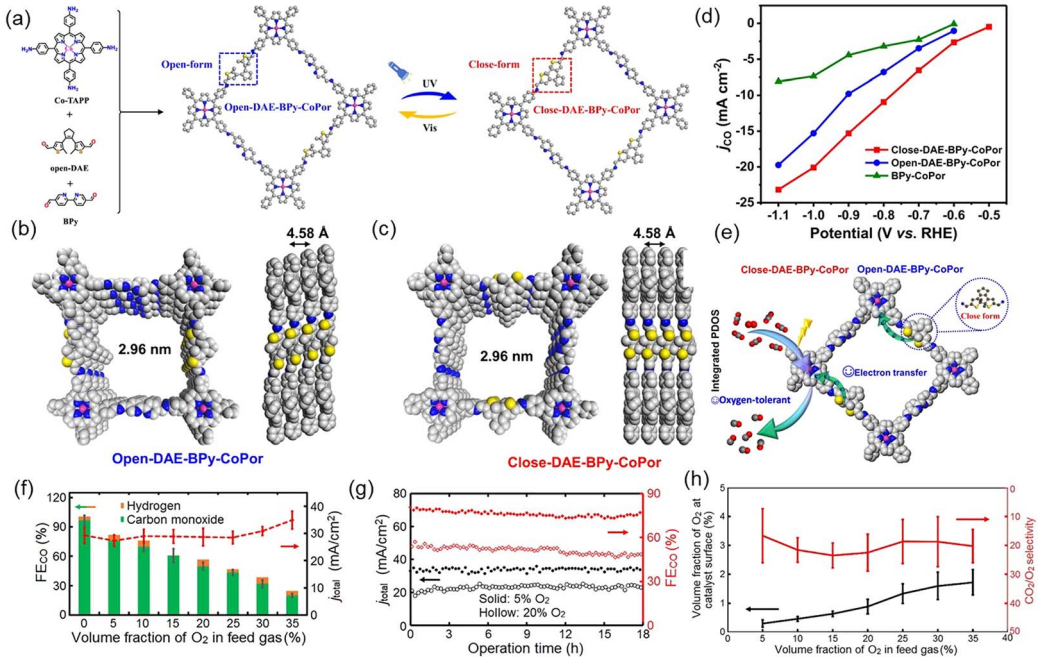

Fig. 3 (a) Synthetic route to open-DAE-BPy-CoPor and close-DAE-BPy-CoPor. Top and side views of (b) open-DAE-BPy-CoPor and (c) close-DAE-BPy-CoPor. (d) The j_{co} of the BPy-CoPor, close-DAE-BPy-CoPor and open-DAE-BPy-CoPor under aerobic conditions. (e) Proposed schematic mechanism for the CO_2RR on close-DAE-BPy-CoPor under aerobic conditions. (f) FE_{CO}, FE_{H2} and j_{total} *vs.* volume fraction of O_2 in the CO_2 feed gas. (g) FE_{CO} and j_{total} during an 18 h electrolysis at O_2 volume fractions of 5% (solid markers) and 20% (hollow markers). (h) Volume fraction of O_2 at the catalyst surface *vs.* that in the feed gas, and CO_2/O_2 selectivity of the PIM gas selection layer in the O_2-tolerant hybrid electrodes. (a–e) Reproduced with permission.[45] Copyright 2024, Springer. (f–h) Reproduced with permission.[41] Copyright 2019, Elsevier.

3.2 Selective CO_2 adsorption

Enhancing the selective CO_2 adsorption on the catalysts by the design of specific morphological structures and surface coating/modification is another effective strategy to gain high-efficiency CO_2RR products in flue gas.

3.2.1 Specific morphological structure. Designing catalysts with specific morphological structures, like microporous architectures with the ability to capture CO_2, is able to promote the CO_2 selective adsorption and reduction. Zhao *et al.*[46] prepared Bi-HHTP with a microporous conductive Bi-based metal–organic framework (Fig. 4), which only showed slightly lower FE_{HCOOH} values in a dilute CO_2 (15 vol%, $CO_2/N_2/O_2$ = 15 : 80 : 5, v/v/v) as the feedstock. Specifically, the FE_{HCOOH} still approached 90% with a current density of 71 mA cm^{-2} at a cell voltage of 2.6 V. It means that the oxygen concentration has a minor effect on the CO_2RR process. The open Bi sites and hydroxyl groups are exposed on the pore surface, playing a role as CO_2 capture and conversion sites. DFT calculations showed that the relatively moderate binding strength of *OCHO on Bi-HHTP made it favorable for further hydrogenation, thus achieving higher CO_2-to-HCOOH selectivity.

3.2.2 Surface coating/modification. Surface coating or modification with alkalic groups can introduce strong chemical affinity to CO_2, a Lewis acid, that realizes selective CO_2 adsorption. For example, Cao *et al.*[47] proposed a polyaniline

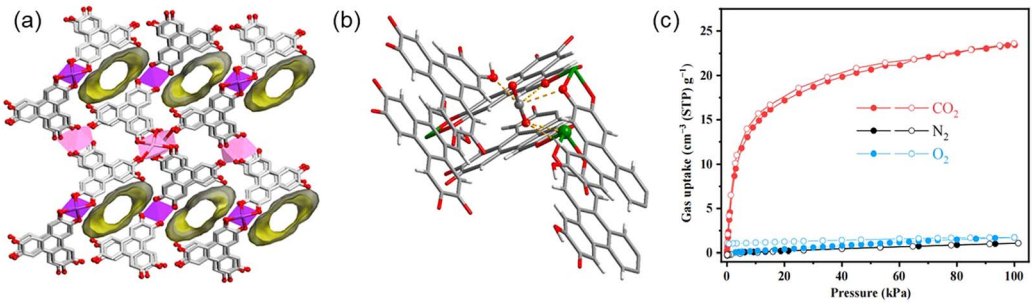

Fig. 4 (a) 3D π–π stacking structure of Bi-HHTP with 1D pores along the *b*-axis direction. (b) The adsorption site for the CO_2 molecule in Bi-HHTP. (c) CO_2, N_2 and O_2 adsorption (solid) and desorption (open) isotherms of Bi-HHTP measured at 298 K, respectively. Reproduced with permission.[46] Copyright 2024, American Chemical Society.

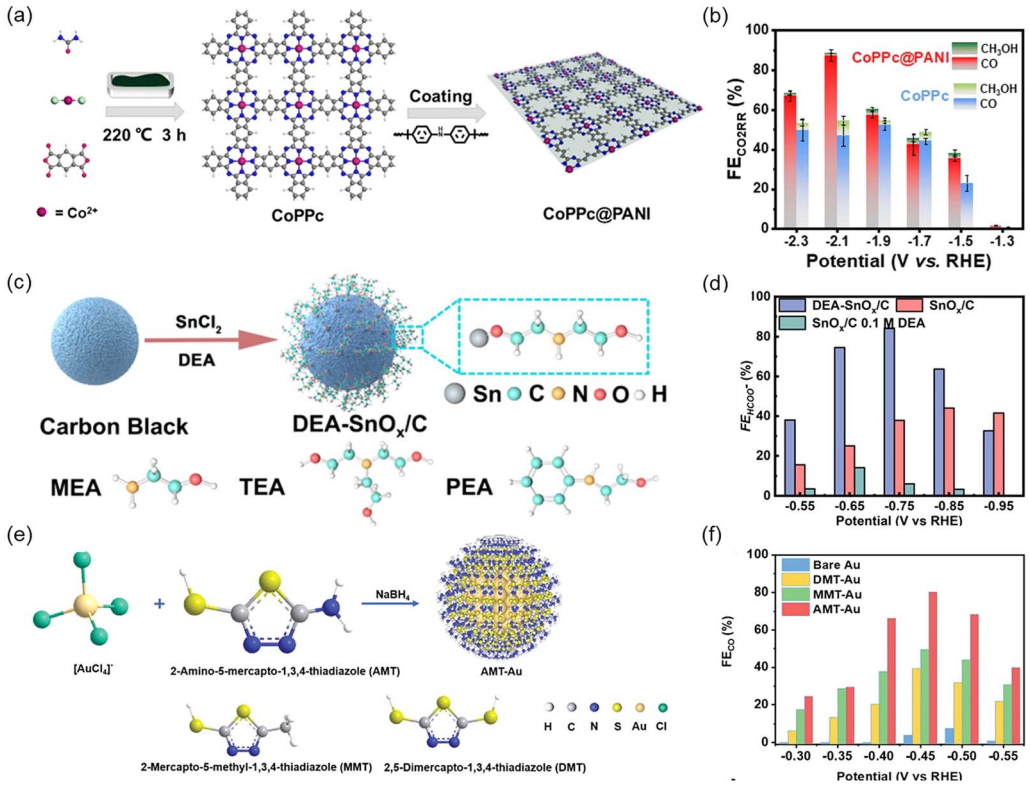

Fig. 5 (a) Schematic illustration of the CoPPc and CoPPc@PANI synthesis. (b) CO_2RR performance between CoPPc@PANI and CoPPc in 5% O_2 and 95% CO_2 feed gas. (c) Fabrication of DEA-SnO_x/C and structures of alkanolamines. (d) FE_{HCOO^-} in 0.5 M $KHCO_3$ electrolyte under simulated flue gas. (e) Scheme of organic ligand modified Au NPs and the structure of organic ligands. (f) FE_{CO} of AMT-Au with pumping simulated flue gas saturated electrolyte in the cathode. (a and b) Reproduced with permission.[47] Copyright 2024, The Royal Society of Chemistry. (c and d) Reproduced with permission.[48] Copyright 2021, American Chemical Society. (e and f) Reproduced with permission.[49] Copyright 2024, Wiley-VCH.

(PANI) coating strategy to achieve highly efficient CO_2RR performance using flue gas in acidic media (Fig. 5a and b). The unique imine groups on PANI can selectively adsorb CO_2 molecules and filter out O_2 molecules near the active Co–N_4 site in the conjugated cobalt polyphthalocyanine framework (CoPPc). Specifically, the acidic CO_2 molecules chemically interact with PANI, allowing faster CO_2 transfer during electrocatalysis compared with CoPPc. Therefore, CoPPc@PANI exhibits a high FE_{CO} of up to 87.4% and an industry-level j_{CO} of -270 mA cm^{-2} at -2.1 V *vs.* RHE under 95% CO_2 + 5% O_2 feed gas in an acidic electrolyte. Similarly, Cheng *et al.*[48] grafted alkanolamines on a tin oxide surface and the surface grafted alkanolamines could selectively enrich CO_2. Therefore, the ORR was inhibited and the reaction intermediates under an aerobic environment were stabilized. A diethanolamine (DEA) modified tin oxide catalyst (DEA-SnO_x/C) (Fig. 5c and d) showed a maximum FE_{HCOO^-} of 84.2% at -0.75 V *vs.* RHE with a j_{HCOO^-} of 6.7 mA cm^{-2} in 0.5 M $KHCO_3$ under simulated flue gas. Another redox-active molecule, 2-amino-5-mercapto-1,3,4-thiadiazole (AMT), was used to functionalize gold nanoparticles (Fig. 5e and f) for CO_2 enrichment by Kang's group recently.[49] The AMT ligand captured CO_2 with strong interaction in the reduced state, but could not capture O_2. Therefore, the ORR was suppressed. The AMT-Au achieved a maximum FE_{CO} of 80.2% at -0.45 V *vs.* RHE in an H-type cell, and 66.0% at a voltage of 2.7 V in a full cell, respectively, with simulated flue gas (15% CO_2, 4% O_2, balanced with N_2). Recently, Sun *et al.*[50] achieved fast, selective CO electrosynthesis directly fed with simulated oxygen-containing flue gas (95% CO_2 + 5% O_2) over the amine-confined Ag catalysts in a flow cell configuration. A FE_{CO} of 84.2% with a j_{CO} of 333.7 mA cm^{-2} was realized by using dimethylamine-modified Ag because amine modification could not only mediate CO_2 adsorption and *COOH intermediate formation but also block the *OOH intermediate pathway in the side reaction of oxygen reduction.

Modification of the pores with strong CO_2 affinity molecules, like amines, can effectively enrich CO_2 and eliminate the influence of O_2. Li *et al.*[51] reported O_2-tolerant catalytic electrodes for CO_2RR by introducing guest aniline molecules into the pores of a PIM layer (Fig. 6). The chemical interaction between the acidic CO_2 molecule and the basic amino group of aniline could selectively capture CO_2, which enhanced CO_2 separation and improved CO_2RR selectivity. The PIM/aniline hybrid electrode achieved a FE_{CO} of 71% with 10% O_2 in the CO_2 feed gas. Infrared spectroscopy measurements validly indicated that CO_2 was likely to be adsorbed by aniline *via* the chemical interaction between the acidic CO_2 and the basic amino group of aniline.

Based on these discussions, local CO_2 enrichment could be realized by introducing functional groups with alkali that can

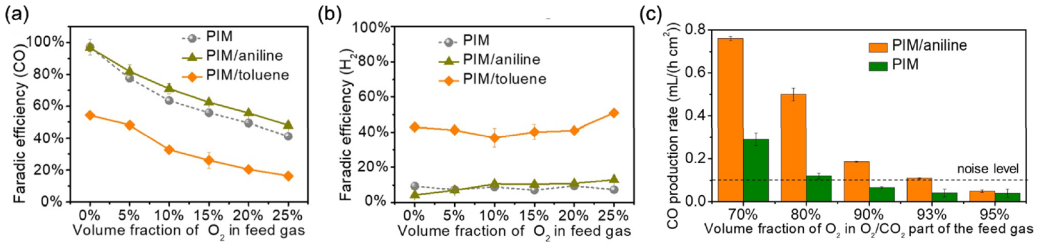

Fig. 6 (a) FE_{CO} and (b) FE_{H2} for PIM, PIM/aniline and PIM/toluene cathodes operating with CO_2/O_2 feed gas containing different O_2 percentages. (c) CO production rate *vs.* volume fraction of O_2 in the O_2/CO_2 part of the feed gas with PIM or PIM/aniline as the CO_2/O_2 selection layer. Reproduced with permission.[51] Copyright 2020, Wiley-VCH.

selectively adsorb CO_2 molecules, or filter the O_2 based on the molecular size, which can enhance the selective reduction of CO_2RR in flue gas.

3.3 Direct selective CO_2RR

Selective CO_2RR in flue gas by designing electrocatalysts with specific electronic structures or optimized electrolyte compositions shall obtain highly selective O_2-tolerant CO_2RR.

3.3.1 Special electronic structure construction. Designing surface active sites with special electronic structures contributes to high CO_2RR performances in the presence of O_2. Recently, an O_2-containing-species coordination strategy to boost CO_2RR in the presence of O_2 was proposed by Cao *et al.*[52] The 2D conjugated COF catalyst (NiPc-Salen$(Co)_2$-COF), which is composed of the Ni-phthalocyanine (NiPc) unit with Ni–N_4–O and the salen$(Co)_2$ moiety with binuclear Co–N_2O_2 sites, exhibited excellent high O_2-tolerant CO_2RR performance and achieved an outstanding FE_{CO} of 97.2% at −1.0 V *vs.* RHE and a high j_{CO} of 40.3 mA cm^{-2} at −1.1 V *vs.* RHE in the presence of 0.5% O_2. The combined ATR-IR and DFT calculations demonstrated that the *OOH of ORR played a significant role in activating CO_2 by enhancing the charge polarization effect, which decreased the free energy of CO_2 activation and boosted the CO_2RR.

3.3.2 Electrolyte optimization. Regulating the electrode/electrolyte interface by choosing an appropriate electrolyte is another key to enhance CO_2RR directly. Acidic media for CO_2RR achieve high carbon utilization efficiency, high overall energy utilization rate, and low carbonate formation, making them a compelling choice for industrial applications.[53] Recently, Wang *et al.* reported that acidic electrolytes have been found to significantly suppress ORR on Cu, enabling generation of multicarbon products from simulated flue gas. By using a Cu composite and carbon supported single-atom Ni as tandem electrocatalysts (Cu PTEE/Ni–N_4), the Cu PTEE/Ni–N_4 achieved a multicarbon FE of 46.5% at 200 mA cm^{-2} in acidic electrolyte,

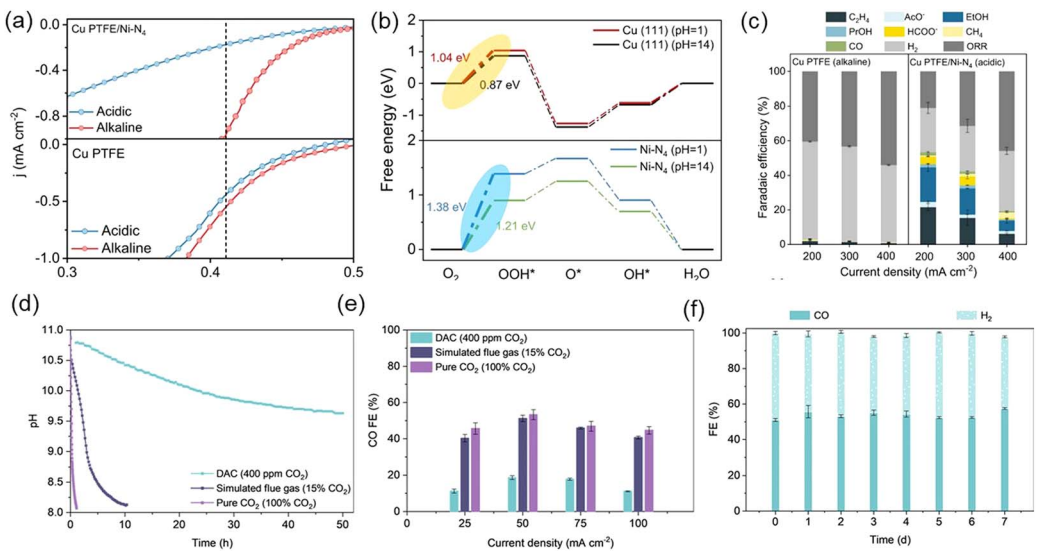

Fig. 7 (a) LSV curves in pure O_2 saturated acidic and alkaline electrolytes. (b) Free energy diagrams of ORR on Ni–N_4 and Cu PTFE at 1.23 V *vs.* SHE. (c) Product FE for Cu PTFE in 1 M KOH and Cu PTFE/Ni–N_4 in 0.05 M H_2SO_4 + 1.5 M Cs_2SO_4 under different current densities. (d) pH of a 2 M K-GLY with 0.1 M KH_2PO_4 capture solution over time while capturing CO_2 from the atmosphere (400 ppm), CO_2 from a simulated flue gas (15%), and pure CO_2 (100%). (e) FE towards CO using the post-capture solutions of the capture processes in (d). (f) FE towards CO and H_2 of a newly assembled electrolyzer while continuously operating at 50 mA cm^{-2} and exposing the same capture solution to 100 sccm of air for 7 days. (a–c) Reproduced with permission.[54] Copyright 2024, Springer. (d–f) Reproduced with permission.[55] Copyright 2024, Springer.

which was ~20 times higher than that of bare Cu under alkaline conditions, enabling O_2-tolerant production of C_{2+} products in simulated flue gas.[54] DFT simulations suggested increases in the free energy change of the rate-determining step for the ORR on Cu and Ni–N_4 tandem sites in acidic media suppressing the ORR (Fig. 7a–c). Additives in the solution can interact with CO_2 molecules, therefore promoting CO_2 enrichment. When using amino acid salts (AAS) as additives, the amino groups can effectively adsorb CO_2 and promote selective CO_2RR. Xiao *et al.*[55] developed a reactive capture strategy using AAS as additives to potassium glycinate capture solution. A maximum FE_{CO} of 19% for direct air capture experiments and a maximum FE_{CO} of 51% for the simulated flue gas experiment were achieved. The CO selectivities for the simulated flue gas and pure CO_2 feed were comparable, demonstrating feasibility of reactive capture with dilute CO_2 inputs when using AAS as the capture solutions (Fig. 7d–f).

4 Summary and outlook

4.1 Summary

Direct CO_2 electroreduction using flue gas (typically containing 3–20% CO_2 and 3–5% O_2) offers a promising route to decarbonize industrial emissions by bypassing energy-intensive capture and purification steps. While strategies like O_2 passivation, selective CO_2 adsorption, and direct CO_2-selective catalysis have advanced aerobic CO_2RR, current research often lacks synthesis of cross-cutting design principles and industrial-relevant performance benchmarks. To bridge this gap, we emphasize two critical directions for practical implementation:

1. Breaking laboratory limits requires targeting the following thresholds. The activity, selectivity and stability parameters of CO_2RR are basic prerequisites for its commercial application. Industrial electrolyzers demand over 200 mA cm^{-2} for current density. In addition, the FE should be higher than 85% with at least 200-hour durability under 5% O_2 coexistence.

2. Multi-impurity tolerance: beyond oxygen challenges. Current research only focuses on a single impurity gas, but the actual situation will be more complex. Different impurity gases, such as SO_2 and NO_2, have varying effects on the system. In addition, smoke may also carry some solid small particles (such as SiO_2, Fe_2O_3, Al_2O_3, CaO, MgO), which may cause side reactions and even lead to the coverage of catalystally active sites. Integrated gas–solid separation could remove most particulates by pre-filtration and preventing active-site coverage.

4.2 Outlook

Despite the effort that has been made in CO_2RR under an aerobic environment, there are still many problems and challenges that need to be addressed for directly feeding with flue gas and applying the industrial-scale CO_2RR.

(i) The relationships among the electrocatalyst, electrolyte, and electrode should be studied. Typically, a more reliable reaction mechanism for effectively regulating the reaction shall be established. Current research on selective CO_2RR remains in its early stages, with only a limited number of studies providing detailed explorations of the underlying mechanisms. Advanced *in situ* characterization techniques and computational methods are also necessary and efficient to obtain more useful information to investigate the structural and physicochemical properties.

(ii) The efficiency of O_2-torelant CO_2RR is important to realize industrial-scale commercial application. The undesirable energy conversion efficiency caused by a high overpotential and low FE limits the near-future practical applications of CO_2RR. Achieving industrial-scale applicability for CO_2/O_2 selective reduction is hindered by the challenge of achieving both high FE and j.[56,57] These performance benchmarks are essential for large-scale applications, but still difficult to satisfy, limiting the potential of directly feeding with flue gas. Additionally, long term stability tests (time > 200 h, j > 200 mA cm^{-2}) shall be studied.

(iii) More attention should be paid to study the selective CO_2RR using low concentration CO_2 condition systems. For example, a typical exhaust gas generated by the combustion of fossil fuels has an O_2/CO_2 ratio of 20%, the coal-fired gas is always composed of 5% O_2, 15% CO_2, 77% N_2 and impurities, and the air contains 20% O_2 and 400 ppm CO_2. Selective O_2/CO_2 reduction using air directly as feed gas can save the cost of CO_2 separation, which is attractive in the future. Therefore, developing electrocatalysts or reactors that can selectively separate and reduce CO_2 directly from CO_2–O_2 mixed gas with various CO_2 contents is crucial.[58–60]

(iv) The economic viability of oxygen–tolerant electrocatalyst manufacturing at an industrial scale faces significant challenges, primarily dictated by process methodology selection. Critical cost drivers—including raw material inputs, post-processing requirements, and waste management—must be holistically optimized, where the choice of synthesis techniques fundamentally determines operational efficiency and environmental impact. For example, electrosynthesis may emerge as a strategic alternative to conventional routes from some aspects. As a direct electrochemical redox platform, it utilizes electricity (ideally sourced from wind/solar) rather than thermal activation, achieving >40% reduction in carbon emissions *versus* thermochemical pathways. Contamination mitigation *via* electrode engineering inherently prevents metal leaching. This eliminates downstream further purification demand.

(v) Industrial-scale CO_2 electroreduction faces system-level challenges beyond catalyst design, necessitating integrated engineering solutions for upstream gas conditioning and downstream product separation. On the upstream side, flue gas containing 3–5% O_2 and particulate impurities competes with CO_2 for catalytically active sites. A multi-stage purification system such as ceramic microfiltration membranes achieves >99% removal efficiency for particulates to prevent catalyst abrasion. Applying a pressure of 3–5 bar elevates local CO_2 concentration >20%, thereby facilitating current densities that surpass the critical industrial benchmark of 200 mA cm^{-2}. On the downstream side, liquid fuels (*e.g.*, formic acid, ethanol) present significant technoeconomic hurdles, particularly due to their dilute nature (<1 mol L^{-1}) in electrolyte-laden catholyte streams (containing K^+/Na^+ species). These challenges manifest

in three primary dimensions: (1) mandatory ion removal through electrodialysis or reverse osmosis processes, which elevate operational expenditures by 30–50%; (2) energy-intensive multi-effect distillation requirements for product concentration, adding 40–60% to the energy balance; and (3) substantially inflated logistics costs combined with the need for additional purification steps to achieve industry-mandated specifications (>90% purity).

Overall, developing electrocatalysts with high CO_2RR ability in flue gas shall shed new light on the development of O_2-tolerant electrocatalysis systems that would facilitate efficient CO_2RR with high activity and selectivity in the presence of O_2. We believe that the CO_2/O_2 selective reduction shall offer new approaches to further improve efficiency and provide novel insights for directly operating CO_2RR under O_2-containing CO_2 feed gas.

Data availability

The sources of the data discussed are all references cited within the article.

Conflicts of interest

There are no conflicts to declare.

Acknowledgements

This work was supported by the Science and Technology Development Fund from Macau SAR (FDCT) (0111/2022/A2, 0050/2023RIB2, 0023/2023/AFJ, 0002/2024/TFP, and 0087/2024/AFJ) and Multi-Year Research Grants (MYRGGRG2023-00010-IAPME and MYRG-GRG2024-00038-IAPME) from Research & Development Office at the University of Macau.

References

1 S. L. Hou, J. Dong and B. Zhao, *Adv. Mater.*, 2020, **32**, 1806163.
2 C. Kim, F. Dionigi, V. Beermann, X. Wang, T. Möller and P. Strasser, *Adv. Mater.*, 2019, **31**, 1805617.
3 Z. Guo, G. Chen, C. Cometto, B. Ma, H. Zhao, T. Groizard, L. Chen, H. Fan, W.-L. Man and S.-M. Yiu, *Nat. Catal.*, 2019, **2**, 801–808.
4 B. M. Tackett, E. Gomez and J. G. Chen, *Nat. Catal.*, 2019, **2**, 381–386.
5 Y. Zhang, J. Zhao and S. Lin, *Chin. J. Struct. Chem.*, 2024, **43**, 100415.
6 Y. X. Xiao, J. Ying, J. B. Chen, X. Yang, G. Tian, J. H. Li, C. Janiak and X. Y. Yang, *Adv. Funct. Mater.*, 2024, **35**, 2418264.
7 R. M. Rodrigues, X. Guan, J. A. Iñiguez, D. A. Estabrook, J. O. Chapman, S. Huang, E. M. Sletten and C. Liu, *Nat. Catal.*, 2019, **2**, 407–414.
8 H. Chen, F. Dong and S. D. Minteer, *Nat. Catal.*, 2020, **3**, 225–244.
9 C. Li, T. Wang, B. Liu, M. Chen, A. Li, G. Zhang, M. Du, H. Wang, S. F. Liu and J. Gong, *Energy Environ. Sci.*, 2019, **12**, 923–928.
10 S. Chen, H. Wang, Z. Kang, S. Jin, X. Zhang, X. Zheng, Z. Qi, J. Zhu, B. Pan and Y. Xie, *Nat. Commun.*, 2019, **10**, 788.
11 J. E. Huang, F. Li, A. Ozden, A. Sedighian Rasouli, F. P. García de Arquer, S. Liu, S. Zhang, M. Luo, X. Wang and Y. Lum, *Science*, 2021, **372**, 1074–1078.
12 J. Feng, J. Li, L. Qiao, D. Liu, P. Zhou, J. Ni and H. Pan, *Appl. Catal., B*, 2023, **330**, 122665.
13 J. Feng, C. Liu, L. Qiao, K. An, S. Lin, W. F. Ip and H. Pan, *Adv. Sci.*, 2024, **11**, 2407019.
14 J. Feng, J. Ni and H. Pan, *J. Mater. Chem. A*, 2021, **9**, 10546–10561.
15 J. Zhao and S. Lin, *J. Colloid Interface Sci.*, 2025, **680**, 257–264.
16 S. Verma, S. Lu and P. J. A. Kenis, *Nat. Energy*, 2019, **4**, 466–474.
17 D. Gao, R. M. Arán-Ais, H. S. Jeon and B. Roldan Cuenya, *Nat. Catal.*, 2019, **2**, 198–210.
18 S. Rasul, A. Pugnant, H. Xiang, J. M. Fontmorin and E. H. Yu, *J. CO2 Util.*, 2019, **32**, 1–10.
19 J. Li, G. Chen, Y. Zhu, Z. Liang, A. Pei, C.-L. Wu, H. Wang, H. R. Lee, K. Liu, S. Chu and Y. Cui, *Nat. Catal.*, 2018, **1**, 592–600.
20 M. Liu, Y. Pang, B. Zhang, P. De Luna, O. Voznyy, J. Xu, X. Zheng, C. T. Dinh, F. Fan, C. Cao, F. P. de Arquer, T. S. Safaei, A. Mepham, A. Klinkova, E. Kumacheva, T. Filleter, D. Sinton, S. O. Kelley and E. H. Sargent, *Nature*, 2016, **537**, 382–386.
21 Q. Lu, J. Rosen, Y. Zhou, G. S. Hutchings, Y. C. Kimmel, J. G. G. Chen and F. Jiao, *Nat. Commun.*, 2014, **5**, 3242.
22 A. Sedighian Rasouli, X. Wang, J. Wicks, G. Lee, T. Peng, F. Li, C. McCallum, C.-T. Dinh, A. H. Ip and D. Sinton, *ACS Sustainable Chem. Eng.*, 2020, **8**, 14668–14673.
23 Y. Chen, J. Zhao, X. Pan, L. Li, Z. Yu, X. Wang, T. Ma, S. Lin and J. Lin, *Angew Chem. Int. Ed. Engl.*, 2024, **63**, e202411543.
24 Y. Xiao, D. Liu, J. Yang, J. Feng, W. Gu, L. Qiao, W. F. Ip and H. Pan, *Nano Lett.*, 2025, **25**, 6548–6555.
25 R. F. Service, *Science*, 2016, **354**, 1362–1363.
26 S. Ren, D. Joulié, D. Salvatore, K. Torbensen, M. Wang, M. Robert and C. P. Berlinguette, *Science*, 2019, **365**, 367–369.
27 D. J. D. Pimlott, A. Jewlal, Y. Kim and C. P. Berlinguette, *J. Am. Chem. Soc.*, 2023, **145**, 25933–25937.
28 S. Xie, C. Deng, Q. Huang, C. Zhang, C. Chen, J. Zhao and H. Sheng, *Angew Chem. Int. Ed. Engl.*, 2023, **62**, e202216717.
29 S. Van Daele, L. Hintjens, S. Hoekx, B. Bohlen, S. Neukermans, N. Daems, J. Hereijgers and T. Breugelmans, *Appl. Catal., B*, 2024, **341**, 123345.
30 D. Tian, Q. Wang, Z. Qu and H. Zhang, *Nano Energy*, 2025, **134**, 110563.
31 K. Williams, N. Corbin, J. Zeng, N. Lazouski, D.-T. Yang and K. Manthiram, *Sustainable Energy Fuels*, 2019, **3**, 1225–1232.
32 T. Al-Attas, S. K. Nabil, A. S. Zeraati, H. S. Shiran, T. Alkayyali, M. Zargartalebi, T. Tran, N. N. Marei, M. A. Al Bari, H. Lin, S. Roy, P. M. Ajayan, D. Sinton, G. Shimizu and M. G. Kibria, *ACS Energy Lett.*, 2022, **8**, 107–115.

33 X. Wen, D. Gao and G. Wang, *ChemSusChem*, 2025, **18**, e202402438.
34 J. J. Li, X. R. Qin, X. R. Wang, L. L. Wang, Z. Y. Yu and T. B. Lu, *ACS Nano*, 2025, **19**, 10620–10629.
35 L. Więcław-Solny, A. Tatarczuk, M. Stec and A. Krótki, *Energy Procedia*, 2014, **63**, 6318–6322.
36 A. A. Basfar, O. I. Fageeha, N. Kunnummal, S. Al-Ghamdi, A. G. Chmielewski, J. Licki, A. Pawelec, B. Tymiński and Z. Zimek, *Fuel*, 2008, **87**, 1446–1452.
37 M. C. Trachtenberg, D. A. Smith, R. M. Cowan and X. Wang, *Flue Gas CO_2 Capture by Means of a Biomimetic Facilitated Transport Membrane*, American Institute of Chemical Engineers, 2007.
38 G. V. Last and M. T. Schmick, *Environ. Earth Sci.*, 2015, **74**, 1189–1198.
39 S. Mondal and S. C. Peter, *Adv. Mater.*, 2024, **36**, 2407124.
40 Y. Zhou, K. Wang, S. Zheng, X. Cheng, Y. He, W. Qin, X. Zhang, H. Chang, N. Zhong and X. He, *Chem. Eng. J.*, 2024, **486**, 150169.
41 X. Lu, Z. Jiang, X. Yuan, Y. Wu, R. Malpass-Evans, Y. Zhong, Y. Liang, N. B. McKeown and H. Wang, *Sci. Bull.*, 2019, **64**, 1890–1895.
42 C. Wilke and P. Chang, *AIChE J.*, 1955, **1**, 264–270.
43 D. Shou, J. Fan, M. Mei and F. Ding, *Microfluid. Nanofluid.*, 2014, **16**, 381–389.
44 Y. Xu, J. P. Edwards, J. Zhong, C. P. O'Brien, C. M. Gabardo, C. McCallum, J. Li, C.-T. Dinh, E. H. Sargent and D. Sinton, *Energy Environ. Sci.*, 2020, **13**, 554–561.
45 H. J. Zhu, D. H. Si, H. Guo, Z. Chen, R. Cao and Y. B. Huang, *Nat. Commun.*, 2024, **15**, 1479.
46 Z. H. Zhao, J. R. Huang, D. S. Huang, H. L. Zhu, P. Q. Liao and X. M. Chen, *J. Am. Chem. Soc.*, 2024, **146**, 14349–14356.
47 L.-Y. Liu, Q. Wu, H. Guo, L. Han, S. Gao, R. Cao and Y.-B. Huang, *J. Mater. Chem. A*, 2024, **12**, 9486–9493.
48 Y. Cheng, J. Hou and P. Kang, *ACS Energy Lett.*, 2021, **6**, 3352–3358.
49 T. Yan, S. Liu, Z. Liu, J. Sun and P. Kang, *Adv. Funct. Mater.*, 2024, **34**, 2311733.
50 J. W. Sun, T. Yu, H. Wu, M. Zhu, A. Chen, C. Lian, H. G. Yang and P. F. Liu, *Chem Catal.*, 2024, **4**, 100923.
51 P. Li, X. Lu, Z. Wu, Y. Wu, R. Malpass-Evans, N. B. McKeown, X. Sun and H. Wang, *Angew Chem. Int. Ed. Engl.*, 2020, **59**, 10918–10923.
52 H. Guo, D. H. Si, H. J. Zhu, Z. A. Chen, R. Cao and Y. B. Huang, *Angew Chem. Int. Ed. Engl.*, 2024, **63**, e202319472.
53 R. Zhang, H. Wang, Y. Ji, Q. Jiang, T. Zheng and C. Xia, *Sci. China: Chem.*, 2023, **66**, 3426–3442.
54 M. Wang, B. Wang, J. Zhang, S. Xi, N. Ling, Z. Mi, Q. Yang, M. Zhang, W. R. Leow, J. Zhang and Y. Lum, *Nat. Commun.*, 2024, **15**, 1218.
55 Y. C. Xiao, S. S. Sun, Y. Zhao, R. K. Miao, M. Fan, G. Lee, Y. Chen, C. M. Gabardo, Y. Yu, C. Qiu, Z. Guo, X. Wang, P. Papangelakis, J. E. Huang, F. Li, C. P. O'Brien, J. Kim, K. Han, P. J. Corbett, J. Y. Howe, E. H. Sargent and D. Sinton, *Nat. Commun.*, 2024, **15**, 7849.
56 T. Burdyny and W. A. Smith, *Energy Environ. Sci.*, 2019, **12**, 1442–1453.
57 D. Wu, F. Jiao and Q. Lu, *ACS Catal.*, 2022, **12**, 12993–13020.
58 A. Elgazzar, P. Zhu, F.-Y. Chen, S. Hao, T.-U. Wi, C. Qiu, V. Okatenko and H. Wang, *ACS Energy Lett.*, 2024, 450–458.
59 A. Prajapati, R. Sartape, M. T. Galante, J. Xie, S. L. Leung, I. Bessa, M. H. S. Andrade, R. T. Somich, M. V. Rebouças, G. T. Hutras, N. Diniz and M. R. Singh, *Energy Environ. Sci.*, 2022, **15**, 5105–5117.
60 B.-U. Choi, Y. C. Tan, H. Song, K. B. Lee and J. Oh, *ACS Sustain. Chem. Eng.*, 2021, **9**, 2348–2357.